

LARGE-SCALE BIOLOGY ARTICLE

# Comprehensive Protein-Based Artificial MicroRNA Screens for Effective Gene Silencing in Plants<sup>W</sup>

Jian-Feng Li,<sup>a,b,1</sup> Hoo Sun Chung,<sup>a,b</sup> Yajie Niu,<sup>a,b</sup> Jenifer Bush,<sup>a,b</sup> Matthew McCormack,<sup>a,b</sup> and Jen Sheen<sup>a,b</sup>

<sup>a</sup> Department of Molecular Biology, Massachusetts General Hospital, Boston, Massachusetts 02114

<sup>b</sup> Department of Genetics, Harvard Medical School, Boston, Massachusetts 02114

ORCID ID: 0000-0001-5783-0804 (J-FL).

**Artificial microRNA (amiRNA) approaches offer a powerful strategy for targeted gene manipulation in any plant species. However, the current unpredictability of amiRNA efficacy has limited broad application of this promising technology. To address this, we developed epitope-tagged protein-based amiRNA (ETPamir) screens, in which target mRNAs encoding epitope-tagged proteins were constitutively or inducibly coexpressed in protoplasts with amiRNA candidates targeting single or multiple genes. This design allowed parallel quantification of target proteins and mRNAs to define amiRNA efficacy and mechanism of action, circumventing unpredictable amiRNA expression/processing and antibody unavailability. Systematic evaluation of 63 amiRNAs in 79 ETPamir screens for 16 target genes revealed a simple, effective solution for selecting optimal amiRNAs from hundreds of computational predictions, reaching ~100% gene silencing in plant cells and null phenotypes in transgenic plants. Optimal amiRNAs predominantly mediated highly specific translational repression at 5' coding regions with limited mRNA decay or cleavage. Our screens were easily applied to diverse plant species, including *Arabidopsis thaliana*, tobacco (*Nicotiana benthamiana*), tomato (*Solanum lycopersicum*), sunflower (*Helianthus annuus*), *Catharanthus roseus*, maize (*Zea mays*) and rice (*Oryza sativa*), and effectively validated predicted natural miRNA targets. These screens could improve plant research and crop engineering by making amiRNA a more predictable and manageable genetic and functional genomic technology.**

## INTRODUCTION

Our knowledge about plant genomes is expanding at an astounding rate, generating an urgent need for techniques that can be used to test the functions of newly uncovered genes. One important test of gene function is the examination of the loss-of-function phenotype. However, generating targeted genetic mutants remains challenging in plants due to the lack of a robust homologous recombination-based approach. Moreover, chemical, physical, and insertional mutagenesis efforts to date have failed to exhaustively cover plant genomes with null mutations (O'Malley and Ecker, 2010). Gene redundancy, lethality, and generating multigene knockouts for genes with close linkage have imposed further challenges to plant genetics and genomic research. Furthermore, the resources requiring intensive mutagenesis approaches may only be available for a limited number of model species and are not sufficient to address gene function in the broad diversity of scientifically, agronomically, and pharmacologically important plant species.

Targeted gene silencing, with its broad adaptability and inducibility, is a potentially valuable tool for gene manipulation and functional analysis in plants. Artificial microRNA (amiRNA) technology, which exploits the biogenesis and silencing machineries

for endogenous microRNAs (miRNAs), enables targeted gene silencing in numerous plant species (Ossowski et al., 2008; Sablok et al., 2011). An amiRNA is built on a native miRNA precursor by replacing the original miRNA-miRNA\* (passenger strand) duplex with a customized sequence. This amiRNA re-directs the miRNA-induced silencing complex to silence the mRNA target of interest, thereby generating a loss-of-function phenotype for the gene of interest (Zeng et al., 2002; Parizotto et al., 2004; Alvarez et al., 2006; Schwab et al., 2006; Ossowski et al., 2008). In plants, silencing requires near-perfect complementarity between the miRNA and its mRNA targets. This ensures superb silencing specificity for plant amiRNAs, in contrast with animal miRNAs, which can modulate hundreds of targets via partial complementarity (Miranda et al., 2006; Chi et al., 2009; Voinnet, 2009; Fabian et al., 2010; Guo et al., 2010; Huntzinger and Izaurralde, 2011; Pasquinelli, 2012). Compared with RNA interference and virus-induced gene silencing, plant amiRNAs have significant advantages, such as minimal off-target effects, unique capacity for multigene silencing, transgenic complementation possibility, and activity at low temperatures (Alvarez et al., 2006; Niu et al., 2006; Schwab et al., 2006; Ossowski et al., 2008).

The Web-based miRNA designer (WMD), which works for more than 100 plant species, allows the design of gene-specific amiRNA candidates within a given transcriptome (Schwab et al., 2006; Ossowski et al., 2008). However, WMD generates hundreds of amiRNA candidates for each target gene and computationally ranks these candidates by sequence complementarity and hybridization energy with unknown *in vivo* efficacy. Indeed, the amiRNA–target interaction can be affected by many *in vivo*

<sup>1</sup> Address correspondence to [jli@molbio.mgh.harvard.edu](mailto:jli@molbio.mgh.harvard.edu).

The author responsible for distribution of materials integral to the findings presented in this article in accordance with the policy described in the Instructions for Authors ([www.plantcell.org](http://www.plantcell.org)) is: Jian-Feng Li ([jli@molbio.mgh.harvard.edu](mailto:jli@molbio.mgh.harvard.edu)).

<sup>W</sup> Online version contains Web-only data.

[www.plantcell.org/cgi/doi/10.1105/tpc.113.112235](http://www.plantcell.org/cgi/doi/10.1105/tpc.113.112235)

factors, including target mRNA structure and mRNA binding proteins (Fabian et al., 2010; Pasquinelli, 2012). Therefore, the optimal amiRNA for silencing is not generally obvious. Numerous other questions also await systematic investigation, and this has limited the broad application of plant amiRNAs. These questions include determining amiRNA specificity, exploring the possibility of using amiRNAs to generate null mutants with complete protein silencing, assessing whether mRNA detection accurately reflects protein silencing by an amiRNA, overcoming the prevailing problem of plant antibody scarcity, deciphering the action mechanisms of amiRNAs in gene silencing, and expanding the applicability of amiRNA to diverse plant species (Alvarez et al., 2006; Schwab et al., 2006; Brodersen et al., 2008; Ossowski et al., 2008; Warthmann et al., 2008; Park et al., 2009; Fabian et al., 2010; Huntzinger and Izaurralde, 2011; Pasquinelli, 2012).

Here, we developed a simple and versatile epitope-tagged protein-based amiRNA (ETPamir) screen to monitor the efficacy, kinetics, mechanism, and specificity of plant amiRNA actions and to circumvent problems in unpredictable amiRNA expression/processing and antibody unavailability. Based on the analyses of 63 WMD-predicted amiRNA candidates in 79 ETPamir screens for 16 genes, we provide novel insights for selecting optimal amiRNAs from hundreds of predicted candidates. These optimal amiRNAs have the potential to reach ~100% protein silencing efficacy for targeting single or multiple genes in protoplasts and transgenic plants. Using ETPamir screens with improved amiRNA guidelines, selection of only three to four amiRNA candidates for each target gene from the WMD output list was generally sufficient to identify optimal amiRNAs. Our results suggest that the prevalent practice of quantifying target mRNA levels fails to accurately reflect the target silencing state, as optimal amiRNAs predominantly mediated highly specific translational repression with limited mRNA decay or cleavage. We further show that ETPamir screens could be easily applied to diverse plant species for optimal amiRNA selection and afford a facile and reliable assessment for predicted plant miRNA targets.

## RESULTS

### ETPamir Screens in *Arabidopsis*

To identify the most potent amiRNAs from hundreds of computationally predicted candidates for a given target gene, we coexpressed individual amiRNA candidates with the target mRNA encoding an epitope-tagged full-length target protein (Figure 1A). For expression, we used *Arabidopsis thaliana* mesophyll protoplasts, which have been demonstrated to have high cotransfection efficiency (Yoo et al., 2007). This strategy directly and rapidly evaluates the ultimate goal of gene silencing at the protein level using commercial antitag antibodies to overcome the widespread paucity of specific plant antibodies.

As a proof of concept, we selected 10 WMD-predicted amiRNA candidates targeting two *Arabidopsis* genes, *MEKK1* (MEK kinase) and *PDS3* (phytoene desaturase), which have well-characterized null mutant phenotypes (Nakagami et al., 2006; Qin et al., 2007). Since WMD computationally ranks putative amiRNA candidates by sequence complementarity and hybridization energy with unknown *in vivo* efficacy, we typically conducted ETPamir screens

with three to four amiRNA candidates, which were chosen from the top of the WMD output list for different target sites within the coding sequence (CDS) of each target gene without potential off-targets (see Supplemental Figures 1A and 1B online). Unlike the animal miRNA target sites that were predominantly found in the 3' untranslated region (UTR) (Chi et al., 2009; Fabian et al., 2010; Huntzinger and Izaurralde, 2011; Pasquinelli, 2012), few plant amiRNA target sites predicted by WMD fell into the UTRs (Schwab et al., 2006; Ossowski et al., 2008). The numerical order of each amiRNA was based on the high-to-low WMD ranking (see Supplemental Figure 1 online).

The hemagglutinin (HA)-tagged target protein, MEKK1-HA or PDS3-HA, was quantified by immunoblot and densitometric analysis using anti-HA antibodies at 18 to 48 h after DNA transfection with or without amiRNA coexpression (Figures 1B and 1D). We observed a substantial reduction of MEKK1-HA protein by its optimal amiRNA, amiR-*MEKK1-3*, at 18 h after cotransfection and near 100% protein silencing by 36 h (Figure 1B, Table 1), and seven tested amiR-*PDS3*s showed a comparable protein reduction trend (Figure 1D, Table 1).

To validate the efficacy of optimal amiRNAs identified by ETPamir screens, we constitutively expressed amiR-*MEKK1-1*, amiR-*MEKK1-3*, amiR-*PDS3-1*, or amiR-*PDS3-4* and compared individual transgenic phenotypes with those of *mekk1* or *pds3* T-DNA insertion null mutants (Nakagami et al., 2006; Qin et al., 2007). Transgenic plants expressing optimal amiR-*MEKK1-3* phenocopied the *mekk1* null mutant, which is seedling lethal, whereas those expressing moderately effective amiR-*MEKK1-1* displayed less severe phenotypes (Figures 1B and 1C). Transgenic plants expressing either amiR-*PDS3-1* or amiR-*PDS3-4* exhibited the same albino phenotype as the *pds3* null mutant (Figure 1E). These data suggested that ETPamir screens faithfully reflect the amiRNA efficacy in multiple transgenic plants.

Although WMD can design gene-specific amiRNA candidates for each target gene, its amiRNA ranking did not predict the experimentally determined ranking, as amiR-*MEKK1-3* was much more potent than amiR-*MEKK1-1* (98% versus 43% silencing efficiency) and all seven amiR-*PDS3*s were considered optimal (91 to 99% silencing efficiency) despite their distinct WMD rankings (Table 1; see Supplemental Figures 1A and 1B online). This is not surprising because the WMD design can only consider the small RNA properties and sequence complementarity, whereas the *in vivo* amiRNA-target interaction can be affected by many unpredictable factors, such as the target mRNA structure and mRNA binding proteins (Fabian et al., 2010; Pasquinelli, 2012). To obtain more comprehensive information about the ETPamir screen and develop new insights for selecting optimal amiRNAs from WMD output lists, we tested other 27 WMD-predicted amiRNAs for silencing seven related or unrelated *Arabidopsis* genes (see Supplemental Figure 2 online). *Arabidopsis* NPK1-related Protein Kinase1 (ANP1), ANP2, ANP3, MAPKKK17, and MAPKKK18 encode closely related but distinct MAP kinase kinases (MAPKKKs), LysM Domain GPI-anchored Protein2 (LYM2) encodes a plasma membrane protein with unclear function, and Zinc Finger of *Arabidopsis Thaliana*6 (ZAT6) encodes a zinc-finger transcription factor. Optimal amiRNAs with 96 to 100% silencing efficacy were identified for all the genes (Table 1;

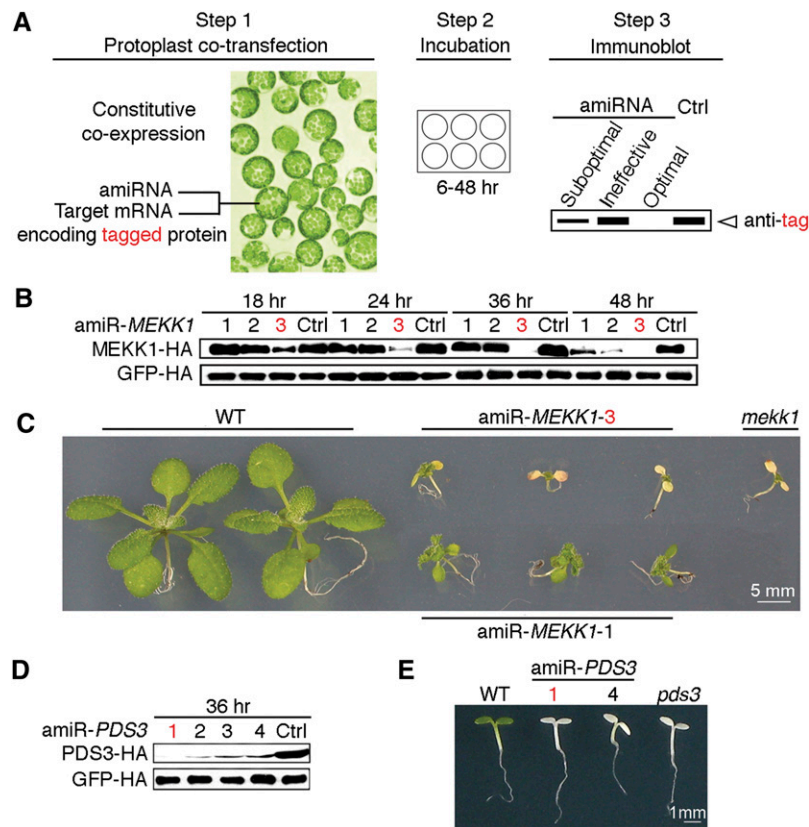


**Figure 1.** ETPamir Screens for Single Gene Silencing in *Arabidopsis*.

**(A)** Scheme of the ETPamir screen. The use of an epitope tag and immunoblot analysis by an antitag antibody for target protein quantification are highlighted in red. The time of protoplast incubation depends on the target protein stability. Empirically, 36 h after cotransfection is an optimal time point to discriminate optimal, moderate, and ineffective amiRNAs for most target genes. Unstable target proteins require shorter incubation time (e.g., 6 to 12 h). Ctrl, control.

**(B)** Time-course immunoblot of MEKK1-HA protein to define optimal amiR-*MEKK1*. The optimal amiRNA, amiR-*MEKK1-3*, is highlighted in red.

**(C)** Transgenic *Arabidopsis* plants overexpressing amiR-*MEKK1-3* resemble the *mekk1* null mutant (SALK\_052557). WT, the wild type.

**(D)** Immunoblot of PDS3-HA protein to define optimal amiR-*PDS3*. The most efficient amiRNA, amiR-*PDS3-1*, is highlighted in red.

**(E)** Transgenic *Arabidopsis* plants overexpressing amiR-*PDS3-1* or amiR-*PDS3-4* resemble the *pds3* null mutant (SALK\_060989).

The numerical order of each amiRNA was based on the high-to-low WMD ranking. In **(B)** and **(D)**, three independent repeats with GFP-HA as an untargeted internal control produced similar results.

see Supplemental Figure 2 online). Although the WMD ranking could not accurately predict optimal amiRNAs defined by ETPamir screens, selection of three to eight candidates for each target gene according to the same rules, namely, from the top of the WMD output list for different target sites within the CDS of each target gene without potential off-targets (see Supplemental Figures 1A and 1B online), was sufficient to identify at least one optimal amiRNA using ETPamir screens (Table 1). As the target protein and amiRNA were produced simultaneously, the stability of the specific target protein and the efficacy of amiRNAs determined the protoplast incubation time (generally 18 to 36 h) required to discriminate optimal, moderate, and ineffective amiRNAs (Figure 1; see Supplemental Figure 2 online). Strikingly, amiR-*ZAT6-1* and amiR-*ZAT6-2* completely blocked target protein accumulation within 6 h after DNA transfection (see Supplemental Figure 2D online), presumably due

to the extremely short half-life (10 min; data not shown) of ZAT6 protein.

### Transgenic Green Fluorescent Protein Sensor for Screening Inducible Gene Silencing

As constitutive expression of optimal amiR-*MEKK1-3* led to early seedling lethality (Figure 1C) that prevented comprehensive studies of silencing mutants in different cell types at various developmental stages, we developed a noninvasive strategy using a constitutively expressed green fluorescent protein (GFP) target sensor (Figure 2A) as a reporter gene to screen for transgenic plants with optimal amiRNA expression induced by estradiol treatment (Zuo et al., 2000). T1 transgenic plants were first screened without estradiol treatment for GFP target sensor expression. T2 transgenic lines expressing the sensor were then

**Table 1.** Summary of AmiRNAs for Single- and Multi-Gene Silencing

AmiRNA <sup>a</sup>	Target Gene	Hybridization Energy (kcal/mol) <sup>b</sup>	Mismatch No. and Position	Target Site/CDS (5' to 3')	WMD Prediction <sup>c</sup>	Silencing Efficiency <sup>d</sup>
<i>MEKK1-1</i>	At4g08500	-33.27 (80.93%)	2 (1, 18)	1142 to 1162/1827	Favorable	43%
<i>MEKK1-2</i>	At4g08500	-36.48 (83.79%)	2 (1, 15)	94 to 114/1827	Favorable	52%
<i>MEKK1-3</i>	At4g08500	-40.16 (98.14%)	2 (1, 21)	199 to 219/1827	Favorable	98%
<i>YDA-1</i>	At1g63700	-37.84 (95.82%)	2 (1, 21)	1752 to 1772/2652	Favorable	82%
<i>YDA-2</i>	At1g63700	-34.18 (88.69%)	2 (1, 21)	2331 to 2351/2652	Favorable	90%
<i>YDA-3</i>	At1g63700	-34.97 (81.67%)	2 (17, 20)	1491 to 1511/2652	Favorable	98%
<i>ALPHA-1</i>	At1g53570	-34.20 (84.17%)	1 (18)	709 to 729/1827	Favorable	90%
<i>ALPHA-2</i>	At1g53570	-37.03 (88.23%)	1 (15)	1512 to 1532/1827	Favorable	99%
<i>ALPHA-3</i>	At1g53570	-37.42 (85.53%)	2 (18, 21)	481 to 501/1827	Favorable	78%
<i>GAMMA-1</i>	At5g66850	-36.16 (91.64%)	2 (1, 15)	1288- to 1308/2151	Favorable	94%
<i>GAMMA-2</i>	At5g66850	-33.66 (82.99%)	1 (17)	126 to 146/2151	Favorable	92%
<i>GAMMA-3</i>	At5g66850	-39.12 (96.69%)	1 (1)	722 to 742/2151	Favorable	100%
<i>ANP1-1</i>	At1g09000	-38.39 (93.98%)	2 (1, 17)	1115 to 1135/2001	Favorable	85%
<i>ANP1-2</i>	At1g09000	-38.73 (95.82%)	1 (21)	1715 to 1735/2001	Favorable	100%
<i>ANP1-3</i>	At1g09000	-40.01 (91.83%)	2 (1, 18)	1407 to 1427/2001	Favorable	80%
<i>ANP2-1</i>	At1g54960	-36.64 (94.31%)	2 (1, 21)	1003 to 1023/1821	Favorable	70%
<i>ANP2-2</i>	At1g54960	-40.62 (93.31%)	1 (20)	1146 to 1166/1821	Favorable	75%
<i>ANP2-3</i>	At1g54960	-38.68 (85.24%)	2 (18, 21)	1375 to 1395/1821	Favorable	83%
<i>ANP2-4</i>	At1g54960	-36.79 (80.68%)	3 (1, 14, 21)	67 to 87/1821	Favorable	41%
<i>ANP2-5</i>	At1g54960	-33.57 (81.30%)	2 (1, 17)	157 to 177/1821	Favorable	99%
<i>ANP2-6</i>	At1g54960	-34.31 (80.88%)	2 (1, 15)	1378 to 1398/1821	Favorable	58%
<i>ANP2-7</i>	At1g54960	-31.74 (83.15%)	2 (18, 21)	1315 to 1335/1821	Favorable	62%
<i>ANP3-1</i>	At3g06030	-38.63 (93.06%)	2 (1, 18)	1288 to 1308/1956	Favorable	75%
<i>ANP3-2</i>	At3g06030	-35.66 (87.96%)	2 (1, 20)	508 to 528/1956	Favorable	99%
<i>ANP3-3</i>	At3g06030	-35.67 (87.58%)	1 (18)	98 to 118/1956	Favorable	70%
<i>3K17-1</i>	At2g32510	-33.62 (84.01%)	2 (1, 18)	382 to 402/1119	Favorable	99%
<i>3K17-2</i>	At2g32510	-38.82 (96.66%)	1 (1)	321 to 341/1119	Favorable	83%
<i>3K17-3</i>	At2g32510	-37.54 (82.11%)	2 (17, 21)	310 to 330/1119	Favorable	89%
<i>3K18-1</i>	At1g05100	-36.95 (95.60%)	2 (1, 21)	656 to 676/1020	Favorable	99%
<i>3K18-2</i>	At1g05100	-38.65 (90.35%)	2 (1, 21)	758 to 778/1020	Favorable	88%
<i>3K18-3</i>	At1g05100	-33.70 (85.49%)	2 (14, 21)	348 to 368/1020	Favorable	ND
<i>LYM2-1</i>	At2g17120	-39.63 (93.40%)	2 (1, 21)	515 to 535/1053	Favorable	31%
<i>LYM2-2</i>	At2g17120	-37.65 (94.08%)	2 (1, 21)	477 to 497/1053	Favorable	45%
<i>LYM2-3</i>	At2g17120	-38.46 (84.10%)	1 (17)	143 to 163/1053	Favorable	96%
<i>LYM2-4</i>	At2g17120	-35.73 (91.87%)	2 (1, 21)	3' UTR	Favorable	94%
<i>LYM2-5</i>	At2g17120	-34.97 (85.67%)	2 (1, 20)	1 to 21/1053	Favorable	78%
<i>LYM2-6</i>	At2g17120	-37.00 (91.88%)	2 (1, 15)	3' UTR	Favorable	81%
<i>LYM2-7</i>	At2g17120	-31.73 (75.75%)	3 (1, 17, 20)	1041 to 1053 + 3' UTR	Favorable	79%
<i>LYM2-8</i>	At2g17120	-40.38 (86.26%)	1 (17)	3' UTR	Favorable	57%
<i>PDS3-1</i>	At4g14210	-36.97 (85.84%)	2 (1, 18)	71 to 91/1701	Favorable	99%
<i>PDS3-2</i>	At4g14210	-36.40 (87.35%)	1 (17)	26 to 46/1701	Favorable	94%
<i>PDS3-3</i>	At4g14210	-38.12 (87.53%)	1 (18)	420 to 440/1701	Favorable	91%
<i>PDS3-4</i>	At4g14210	-39.48 (92.61%)	2 (1, 20)	1447 to 1467/1701	Favorable	91%
<i>PDS3-5</i>	At4g14210	-37.02 (81.42%)	2 (1, 17)	71 to 91/1701	Favorable	97%
<i>PDS3-6</i>	At4g14210	-41.81 (93.18%)	2 (1, 20)	71 to 91/1701	Less favorable	93%
<i>PDS3-7</i>	At4g14210	-42.62 (98.45%)	1 (1)	71 to 91/1701	Unfavorable	94%
<i>ZAT6-1</i>	At5g04340	-41.00 (94.34%)	2 (1, 18)	429 to 449/717	Favorable	93%
<i>ZAT6-2</i>	At5g04340	-38.96 (92.63%)	2 (1, 21)	537 to 557/717	Favorable	100%
<i>ZAT6-3</i>	At5g04340	-36.49 (82.09%)	2 (1, 14)	429 to 449/717	Favorable	31%
<i>ZAT6-4</i>	At5g04340	-34.33 (85.33%)	2 (1, 18)	333 to 353/717	Favorable	85%
<i>ZAT6-5</i>	At5g04340	-33.99 (87.31%)	1 (15)	142 to 162/717	Favorable	69%
<i>GFP-1</i>	<i>GFP</i>	-51.48 (92.46%)	1 (1)	529 to 549/720	Less favorable	ND
<i>GFP-2</i>	<i>GFP</i>	-48.46 (91.00%)	1 (1)	72 to 92/720	Unfavorable	ND
<i>GFP-3</i>	<i>GFP</i>	-47.50 (90.74%)	1 (1)	283 to 303/720	Unfavorable	ND
<i>GFP-4</i>	<i>GFP</i>	-42.82 (92.48%)	1 (1)	441 to 461/720	Unfavorable	95%
<i>RACK1-1</i>	At1g48630	-37.78 (70.02%)	3 (1, 15, 17)	961 to 981/981	Less favorable	ND
	At1g18080	-31.78 (70.02%)	3 (1, 15, 17)	964 to 984/984		ND

(Continued)

**Table 1.** (continued).

AmiRNA <sup>a</sup>	Target Gene	Hybridization Energy (kcal/mol) <sup>b</sup>	Mismatch No. and Position	Target Site/CDS (5' to 3')	WMD Prediction <sup>c</sup>	Silencing Efficiency <sup>d</sup>
<i>RACK1-2</i>	At3g18130	-31.78 (70.02%)	3 (1, 15, 17)	961 to 981/981		54%
	At1g48630	-37.10 (83.62%)	3 (5, 17, 20)	2 to 22/981	Less favorable	97%
	At1g18080	-38.24 (86.18%)	2 (17, 20)	2 to 22/984		89%
<i>RACK1-3</i>	At3g18130	-39.12 (88.17%)	3 (5, 14, 20)	2 to 22/981		68%
	At1g48630	-36.09 (77.58%)	2 (15, 17)	365 to 385/981	Less favorable	85%
	At1g18080	-34.45 (74.05%)	2 (8, 15)	365 to 385/984		77%
<i>RACK1-4</i>	At3g18130	-36.09 (77.58%)	2 (15, 17)	365 to 385/981		61%
	At1g48630	-41.43 (94.94%)	2 (1, 21)	179 to 199/981	Less favorable	99%
	At1g18080	-42.53 (97.46%)	2 (1, 21)	179 to 199/984		98%
	At3g18130	-40.88 (93.68%)	4 (1, 2, 20, 21)	179 to 199/981		91%

See Supplemental Figure 11 online for a visual summary of Table 1.

<sup>a</sup>The numerical order of each amiRNA is based on the high-to-low WMD ranking.

<sup>b</sup>The number in parentheses = hybridization energy of the amiRNA to the target site/that of the amiRNA to a perfect complement  $\times 100\%$ .

<sup>c</sup>WMD categorizes predicted amiRNA candidates based on sequence complementarity and hybridization energy.

<sup>d</sup>Efficiency is calculated by densitometric analysis of immunoblot signals (36 h) of ETPamir screens and is presented as the mean value of at least three independent repeats. ND, No detectable gene silencing.

germinated on the estradiol-containing medium to transiently trigger amiR-*MEKK1-3* expression, and those with optimal amiRNA expression could be easily identified by the loss of GFP fluorescence within 48 h after germination (Figure 2B) and be rescued to plates without estradiol for GFP reexpression and plant recovery. By contrast, T2 transgenic lines with unsuccessful silencing retained GFP fluorescence (Figure 2B). The T2 lines with successful silencing could then be induced to express amiR-*MEKK1-3* by estradiol for examining *mekk1* null phenotypes at desirable developmental stages and in specific organs. The identified transgenic plants with optimal inducible silencing grew normally without estradiol (data not shown) but exhibited early senescence and lethality resembling the *mekk1* null mutant after prolonged estradiol treatment (Figure 2C).

The *mekk1* null phenotypes and complete loss of GFP fluorescence in transgenic silencing plants induced by estradiol were validated by the depletion of MEKK1 and GFP-Target<sub>amiR-MEKK1-3</sub> proteins (Figure 2D). However, *MEKK1* and GFP-Target<sub>amiR-MEKK1-3</sub> transcript levels were differentially reduced (22 and 85%, respectively) by amiR-*MEKK1-3*. As the 35S-driven GFP-Target<sub>amiR-MEKK1-3</sub> was expressed at a significantly higher level than the endogenous *MEKK1* (Figure 2D), this dramatic difference and/or the distinct locations or/and different sequence contexts of the amiR-*MEKK1-3* target sequence in two target transcripts (Figure 2D) could probably influence amiRNA regulatory mechanisms. Our data demonstrated the value of using the GFP target sensor for transgenic screens for amiRNAs that give optimal silencing and suggested that quantifying steady state target mRNA levels does not accurately reflect the actual protein silencing state. It is likely that multiple pathways can regulate amiRNA-mediated protein and mRNA silencing (Fukaya and Tomari, 2012), which require further kinetic and mechanistic analyses.

### Single Optimal AmiRNA for Multigene Silencing

To test whether the ETPamir screen could also facilitate the identification of optimal amiRNAs for multigene silencing, we

selected two multigene families, the *RECEPTOR FOR ACTIVATED C KINASE1 (RACK1)* family (*RACK1a*, *RACK1b*, and *RACK1c*) and the *MAPKKK YDA* family (*ALPHA*, *YDA*, and *GAMMA*), for their complex roles in stress and immune signaling pathways (MAPK Group, 2002; Guo and Chen, 2008; Ren et al., 2008). We chose four WMD-predicted amiRNAs to silence each gene family despite their classification in the less favorable or unfavorable category by WMD (see Supplemental Figures 3A and 3B online). Interestingly, among the four amiR-*RACK1*s for *RACK1a/1b/1c*, only amiR-*RACK1-4* could reproducibly achieve potent silencing (91 to 99% efficiency) of the three *RACK1* genes (Figures 3A and 3B, Table 1). The WMD-predicted top candidate amiR-*RACK1-1* was only moderately effective in silencing *RACK1c* (Figure 3B, Table 1). Constitutive expression of amiR-*RACK1-1* or amiR-*RACK1-4* in transgenic *Arabidopsis* confirmed the same efficacy defined by ETPamir screens. Multiple transgenic plants expressing amiR-*RACK1-1* had no overt phenotypes, but those expressing amiR-*RACK1-4* showed a markedly stunted phenotype, closely resembling the *rack1a,1b,1c* triple null mutant (Guo and Chen, 2008) (Figure 3C). These transgenic data again demonstrated the robustness of ETPamir screens in accurately reflecting amiRNA efficacy in planta.

None of the four *YDA* family-specific amiRNA candidates (amiR-AYGs) was effective in ETPamir screens (Figure 4A; see Supplemental Table 1 online). This failure was not due to the lack of amiRNA expression or proper processing, as RNA gel blot analysis detected similar mature amiRNAs (see Supplemental Figure 4 online). Although the expression levels of amiR-*LYM2-3* and amiR-*GFP-4* were not the highest, they exerted 95 to 96% protein silencing, whereas the highly expressed amiR-*LYM2-2* and amiR-*GFP-2/3* only showed 0 to 45% protein silencing (see Supplemental Figure 4 online; Table 1), suggesting that there is no simple correlation between amiRNA levels and their efficacies (Schwab et al., 2006). Importantly, ETPamir screens always identified optimal amiRNAs with effective expression and processing not predictable by WMD (see Supplemental Figure 4 online). Sequence alignment revealed more significant sequence divergence

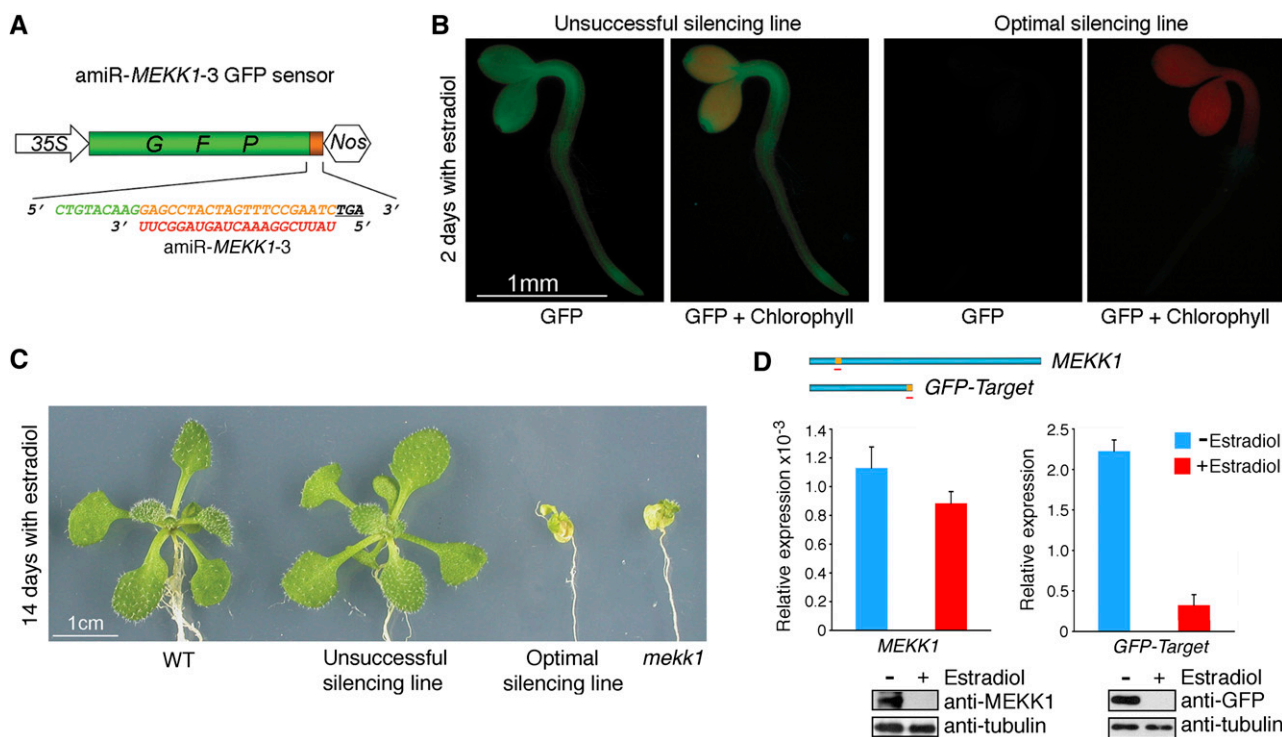


**Figure 2.** Visual GFP-Target Sensor Screen for Transgenic Plants with Optimal Inducible Silencing.

**(A)** Schematic diagram of the GFP target sensor for amiR-*MEKK1-3*. The amiRNA target sequence (orange) was inserted between *GFP* (green) and the stop codon (underlined). The amiRNA sequence is shown in red.

**(B)** GFP sensor expression oppositely reflects amiR-*MEKK1-3* expression. Expression of amiR-*MEKK1-3* was induced by 10  $\mu$ M estradiol in transgenic *Arabidopsis* seedlings constitutively expressing the GFP sensor.

**(C)** Identified transgenic lines with optimal inducible silencing exhibit the *mekk1* null phenotypes after prolonged estradiol treatment. WT, the wild type.

**(D)** Uncoupled protein and mRNA levels for *MEKK1* and *GFP-target* in transgenic silencing plants. The location of the amiR-*MEKK1-3* (red line) target site in both target transcripts is shown in orange. Transcript abundances of *MEKK1* and *GFP-target* in 14-d-old optimal silencing plants with (red) or without (blue) estradiol treatment were quantified by qRT-PCR with amplicons spanning the amiRNA target site. The quantitative PCR data represent means  $\pm$  SD of at least three independent repeats with *UBQ10* expression level set as 1. Parallel examination of target protein levels was conducted by immunoblotting using anti-*MEKK1* and anti-GFP antibodies, respectively, with tubulin as an internal control. Due to the low affinity of anti-*MEKK1* antibody, *MEKK1* proteins in seedling crude extracts were first enriched by immunoprecipitation before immunoblot analysis.

in the *YDA* family compared with the *RACK1* family (see Supplemental Figure 3C online), which might indicate an intrinsic difficulty in silencing multiple genes with limited sequence identity using a single amiRNA.

#### Polycistronic or Tandem AmiRNAs for Multigene Silencing

As the four inactive amiR-AYGs represented the only available *YDA* family-specific candidates from the WMD output list (see Supplemental Figure 3B online), we decided to first identify individual optimal amiRNAs for each gene using the simple and effective ETPamir screens (Figure 4B; see Supplemental Figure 5 online). We then compared two strategies, polycistronic or tandem expression of optimal amiRNAs, for multigene silencing. The polycistronic strategy generated multiple amiRNAs from a single transcript (Figure 4C), which was inspired by the polycistronic miRNAs found in nature (Merchan et al., 2009) and has been successfully employed to silence viral RNA in transgenic plants (Niu et al., 2006). We also developed the tandem strategy

to express multiple amiRNAs separately for potentially more efficient amiRNA expression and processing (Figure 4C). To facilitate ETPamir screens of multigene silencing in the same cell, we introduced a reporter system dubbed “SUMO ladder” (Figure 4D), which represented three different target reporter proteins composed of one, two, or three copies of the small ubiquitin-like modifier (SUMO) and each carried a different amiRNA target sequence before the HA tag CDS (Figure 4D). Coexpression of the SUMO ladder designed for the *YDA* family with individual optimal amiRNAs specifically eliminated a corresponding target reporter (Figure 4E), illustrating the specificity of ETPamir screens. Notably, coexpression of the SUMO ladder with either polycistronic or tandem optimal amiRNAs led to simultaneous silencing of all three reporters (Figure 4E). The effectiveness of polycistronic and tandem optimal amiRNAs was further confirmed by the significant silencing of full-length *YDA* family members in tobacco (*Nicotiana benthamiana*) leaves through *Agrobacterium tumefaciens*-mediated coinfiltration (see Supplemental Figures 6A and 6B online). Our data suggested that both strategies enable efficient

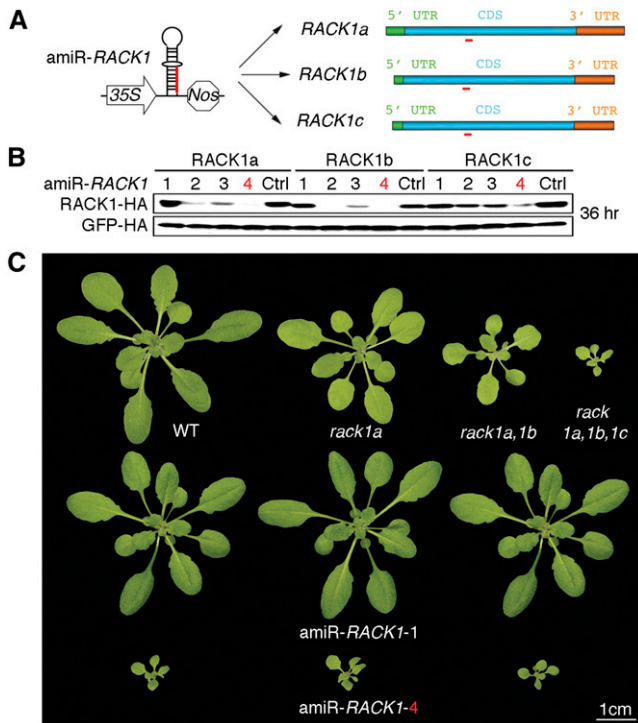


**Figure 3.** Multiple Gene Silencing in *Arabidopsis* by a Single Optimal AmiRNA.

(A) Schematic diagram of amiR-*RACK1* (red) for silencing three target genes, *RACK1a*, *1b*, and *1c*, of the *RACK1* family.

(B) Immunoblot of RACK1-HA proteins to define optimal amiR-*RACK1*. The numerical order of each amiRNA was based on the high-to-low WMD ranking, and the optimal amiR-*RACK1-4* is highlighted in red. Three independent repeats with GFP-HA as an untargeted internal control produced similar results. Ctrl, control.

(C) Transgenic *Arabidopsis* plants overexpressing amiR-*RACK1-4* resemble the *rack1a, 1b, 1c* triple null mutant. WT, the wild type.

silencing of multiple targets with low sequence identity and provide novel tools for future functional analyses of MAPKKKs.

### Predominant Translational Repression by Optimal AmiRNAs

Our parallel quantification of *MEKK1* and *GFP-target<sub>amiR-MEKK1-3</sub>* transcripts and proteins in transgenic silencing plants did not support a tight correlation between the steady state target mRNA level and protein abundance (Figure 2). To dissect the relative contributions of target mRNA cleavage, mRNA decay, and translational repression to amiRNA-mediated gene silencing, we investigated the kinetics and mechanism of amiRNA action within an early time frame after target mRNA expression. This was accomplished by constitutively expressing the amiRNA, but expressing the target mRNA under the control of a heat shock promoter (Figure 5A). Within 3 h after the 1-h target mRNA induction pulse, the same optimal amiRNA for *MEKK1*, *PDS3*, or *RACK1a/1b/1c* was identified (Figures 5B to 5D) as in the screens with constitutive target mRNA and amiRNA coexpression for 36 h (Figures 1 and 3).

We then quantitatively monitored and compared the target mRNA level and protein abundance within 1 to 3 h after the target mRNA induction pulse (Figure 5A) for 11 optimal amiRNAs. Target protein quantification was conducted 2 h after target mRNA quantification to allow more time for protein translation. The target mRNA level showed little change during this 2-h period (data not shown). We observed that all optimal amiRNAs mediated target gene silencing through a combination of translational repression and mRNA decay without a strict correlation (Figure 5E). Unexpectedly, we found no evidence for high levels of accumulation of target mRNA cleavage products as quantitative RT-PCR (qRT-PCR) amplicons upstream, downstream, or spanning the potential mRNA cleavage sites showed comparable levels (Figures 5A and 5E). For most of the optimal amiRNAs, translational repression appeared to play a major role in gene silencing because a dramatic reduction of target protein occurred in the presence of significantly discernible target transcripts (Figure 5E). In particular, as we observed in transgenic studies (Figure 2D), similarly high levels of *MEKK1* transcripts were detected in protoplasts despite nearly complete protein silencing by amiR-*MEKK1-3* (Figure 5E). Our findings agree with previous reports on the translational repression by plant miRNAs (Aukerman and Sakai, 2003; Chen, 2004; Gandikota et al., 2007; Brodersen et al., 2008; Dugas and Bartel, 2008). The generally limited availability of specific plant antibodies has hindered studies on protein silencing by plant amiRNAs, and gene silencing through translational inhibition by plant amiRNAs has been largely overlooked.

### Highly Specific Gene Silencing by Plant AmiRNAs

The WMD offers a superior platform to design gene-specific amiRNAs based on sequence complementarity in a transcriptome context. Previous genome-wide transcript profiling suggested highly specific gene silencing by plant amiRNAs at the mRNA level (Schwab et al., 2006; Ossowski et al., 2008). As amiRNA-mediated gene silencing could occur predominantly through translational inhibition with little alteration of target mRNA levels (Figure 5E), ETPamir screens might offer a more accurate evaluation of gene silencing specificity at the protein level. Our studies of the SUMO reporters with distinct amiRNA target sequences matching three different amiRNAs supported stringent specificity of amiRNA in protein silencing (Figure 4E). We further examined three optimal amiRNAs for the three full-length genes of the MAPKKK YDA family and showed that highly specific protein silencing was achieved for these related genes (see Supplemental Figure 7A online). Surprisingly, an amiRNA that efficiently silenced *ZAT6* was completely inactive in silencing the closely related *ZAT10*, even though the amiRNA only had a mismatch at the position 19 (see Supplemental Figure 7B online), which was usually considered uncritical (Schwab et al., 2005, 2006). These results further supported the value of ETPamir screens for experimental validation of amiRNA efficacy and specificity.

### ETPamir Screens in Diverse Plant Species

To determine whether ETPamir screens could also be applied to diverse plant species, we first evaluated the efficacy of four amiR-GFPs (see Supplemental Figure 1C online) for silencing *GFP* in *Arabidopsis* mesophyll protoplasts. We identified amiR-*GFP-4* as

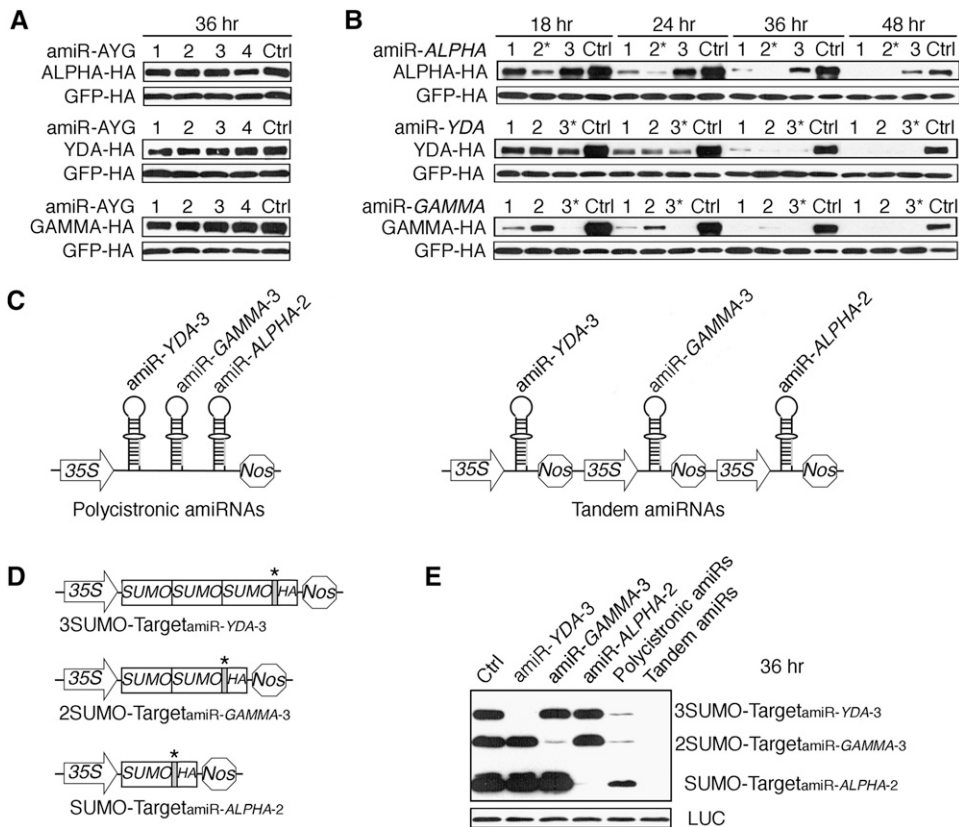


**Figure 4.** Multiple Gene Silencing in *Arabidopsis* by Polycistronic or Tandem Optimal AmiRNAs.

**(A)** ETPamir screens fail to identify an optimal amiRNA (amiR-AYG) for silencing three target genes, *ALPHA*, *YDA*, and *GAMMA*, of the *MAPKKK YDA* family. Ctrl, control.

**(B)** Time-course immunoblots from ETPamir screens for optimal amiRNAs silencing individual genes of the *YDA* family. The most efficient amiRNAs are marked by asterisks.

**(C)** Schematic diagrams of polycistronic or tandem optimal amiRNAs.

**(D)** Schematic diagrams of SUMO ladder reporters for simultaneously screening multiple target silencing in the same cell. Cognate amiRNA target sequence (gray) sensitizing each reporter to a specific amiRNA was inserted in front of the HA tag CDS and is marked by an asterisk.

**(E)** Both polycistronic and tandem optimal amiRNAs can significantly cosilence the *YDA* family.

The numerical order of each amiRNA was based on the high-to-low WMD ranking. In **(A)**, **(B)**, and **(E)**, five independent repeats with GFP-HA or luciferase (LUC) as an untargeted internal control obtained similar results.

the only potent amiR-*GFP* (Figure 6A, Table 1), despite its very low WMD ranking (see Supplemental Figure 1C online). Live-cell imaging further confirmed that a 3-h preexpression of amiR-*GFP-4* but not amiR-*GFP-1* suppressed the subsequent nuclear *GFP* (*NLS-GFP*) expression induced by 1 h of heat shock treatment (Figure 6B). Moreover, amiR-*GFP-4* but not other amiR-*GFPs* significantly blocked GFP expression in tobacco leaves after *Agrobacterium*-mediated coinfiltration (see Supplemental Figure 6C online).

We then gauged the efficacy of amiR-*GFP-4* in transiently transfected mesophyll protoplasts from several dicot and monocot plants, including tobacco, tomato (*Solanum lycopersicum*), sunflower (*Helianthus annuus*), *Catharanthus roseus*, maize (*Zea mays*), and rice (*Oryza sativa*). Although the heat shock promoter (*HSP18.2*) and the miR319a backbone used in ETPamir screens were both derived from *Arabidopsis*, we could readily identify amiR-*GFP-4* as the optimal amiR-*GFP* in all tested plant species except rice (Figure 6C). Although the *Arabidopsis* miR319a-derived amiR-

*GFP-4* had dramatically reduced activity in rice (see Supplemental Figure 8A online), the rice miR528-derived (Warthmann et al., 2008) amiR-*GFP-4* could be identified as the optimal amiRNA for silencing *GFP* in rice using ETPamir screens (Figure 6D). Interestingly, the rice miR528-derived amiR-*GFP-4* also had rather weak activity in *Arabidopsis* (see Supplemental Figure 8B online). Therefore, despite a certain level of cross-species activity in the expression and processing of plant amiRNAs derived from an exogenous miRNA backbone, it is perhaps most desirable to use the amiRNA backbone derived from the same or closely related plants to achieve optimal gene silencing in a given plant species.

#### Unlimited Argonaute Activity in *Arabidopsis* Mesophyll Protoplasts

Argonaute (AGO) proteins are catalytic components of the miRNA-induced silencing complex that is responsible for gene



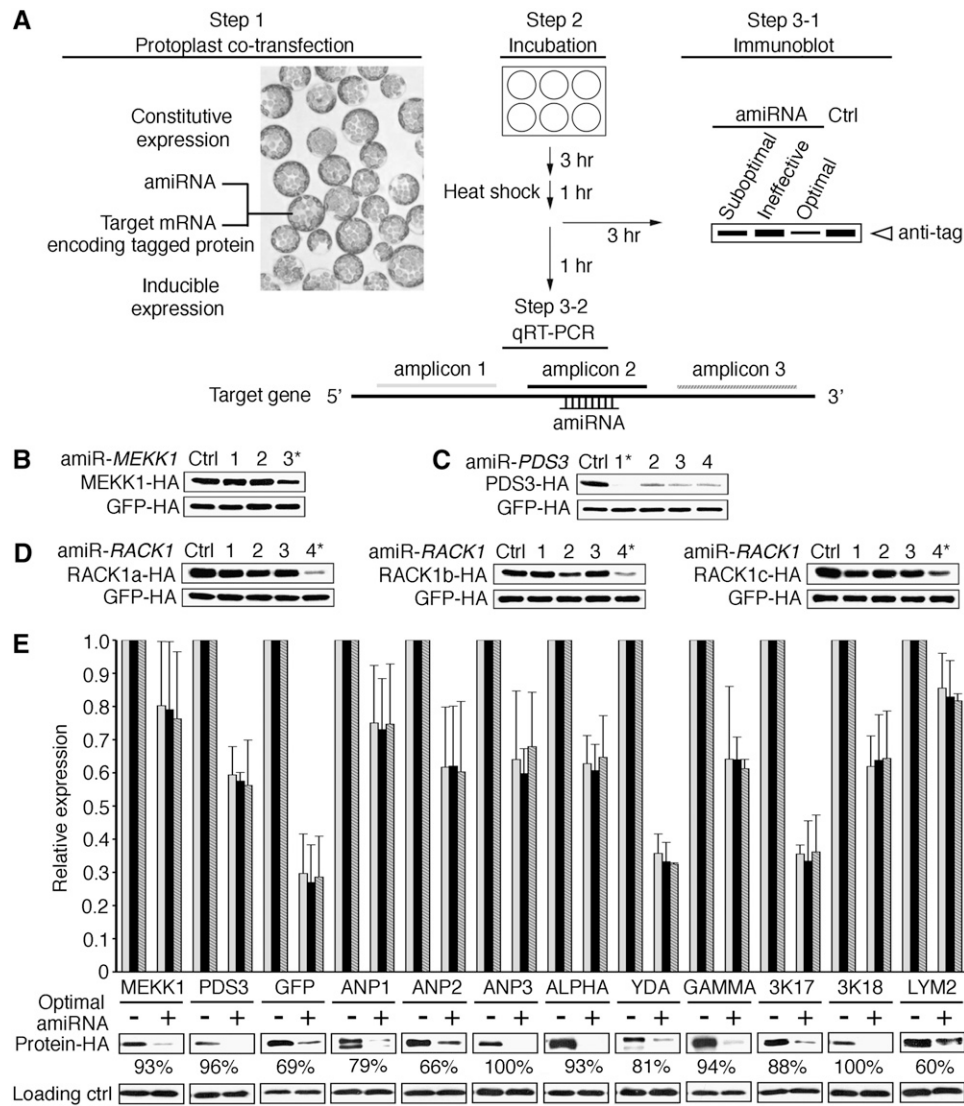


**Figure 5.** Optimal AmiRNAs Act Predominantly via Translational Repression.

**(A)** Scheme of the rapid ETPamir screen. AmiRNA candidates were constitutively expressed, whereas the target mRNAs were expressed under the control of heat shock promoter. Ctrl, control.

**(B)** Quantification of MEKK1-HA protein 3 h after heat shock. The most efficient amiRNAs are marked by asterisks.

**(C)** Immunoblot of PDS3-HA protein 3 h after the heat shock pulse.

**(D)** Immunoblot of RACK1-HA proteins 3 h after the heat shock pulse.

**(E)** Parallel quantification of target transcripts by qRT-PCR and target proteins by immunoblot. The qRT-PCR was conducted with at least three biological repeats using three pairs of primers as shown in **(A)**, aiming at the 5' end (light gray), the amiRNA target site (black), and the 3' end (dark gray with white stripes), respectively, within the CDS of the target gene. The quantitative PCR data obtained using the same pair of primers were first normalized against *UBQ10* expression levels before they were used to determine the relative transcript levels of each target gene with or without silencing. The efficacy of protein silencing was calculated based on densitometric analysis of immunoblot signals of at least three independent repeats and is presented as the mean value. In **(B)** to **(E)**, at least three independent repeats with heat shock-inducible GFP-HA (or LUC for GFP silencing) as an internal control produced similar results.

silencing (Fabian et al., 2010; Huntzinger and Izaurralde, 2011). We addressed the question whether coexpression of the four AGO genes (i.e., *AGO1*, 2, 4, and 10) naturally expressed in *Arabidopsis* mesophyll protoplasts could further enhance the target gene silencing in ETPamir screens. When the target mRNA (*MEKK1* or *GFP*) and its corresponding amiRNAs were constitutively coexpressed, obvious protein

silencing could be detected at 8 h after DNA transfection in the presence of optimal amiRNAs (see Supplemental Figures 9A and 9B online). Coexpression of the AGO genes did not significantly enhance the gene silencing efficacy for optimal or suboptimal amiRNAs (see Supplemental Figure 9 online), suggesting that *Arabidopsis* mesophyll protoplasts have sufficient AGO activities.

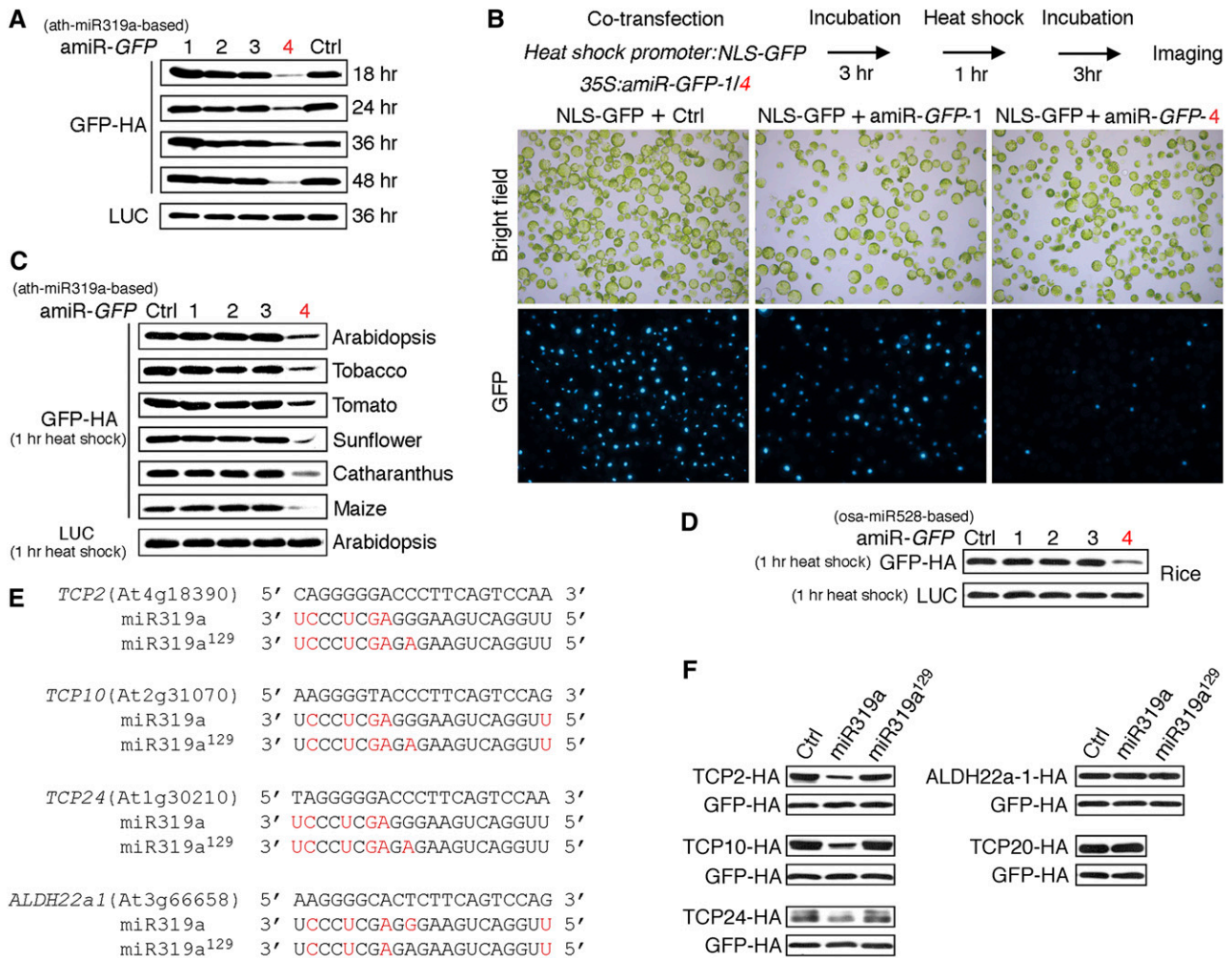


**Figure 6.** Broad Adaptability and Versatility of the ETPamir Screen.

**(A)** Time-course ETPamir screens for optimal amiRNA silencing *GFP* (35S-driven) in *Arabidopsis* mesophyll protoplasts. The numerical order of each amiR-*GFP* was based on the high-to-low WMD ranking. Luciferase (LUC) expression served as an internal control. Ctrl, control.

**(B)** Preexpression of amiR-*GFP*-4 but not amiR-*GFP*-1 suppresses *GFP* expression. As shown by the flow diagram, expression of nuclear *GFP* (NLS-*GFP*) was induced by a 1-h heat shock pulse after 3 h of constitutive expression of amiR-*GFP*s in *Arabidopsis* protoplasts. Images of NLS-*GFP* with ~300, 150, and 180 cells are shown from left to right.

**(C)** Rapid ETPamir screens in protoplasts from diverse plant species. Expression of *GFP* was induced by a 1-h heat shock pulse after 3 h of constitutive expression of amiR-*GFP*s. Heat shock-inducible LUC served as an internal control.

**(D)** Rapid ETPamir screens in rice protoplasts. Expression of *GFP* was induced by a 1-h heat shock pulse after 3 h of constitutive expression of amiR-*GFP*s. Unlike the amiR-*GFP*s in **(A)** to **(C)** that were derived from *Arabidopsis* miR319a (ath-miR319a), amiR-*GFP*s derived from rice miR528 (osa-miR528) were used.

**(E)** Sequence alignment between miR319a and putative target sites. Mismatches in miR319a or miR319a<sup>129</sup> (nonfunctional variant) to individual predicted target sequences are highlighted in red.

**(F)** Validation of predicted target genes for miR319a using protein-based miRNA target screens. Expression of target candidates was induced by a 1-h heat shock pulse after 3 h of constitutive expression of miR319a or miR319a<sup>129</sup>. *TCP20*, as a known untargeted gene, was tested as a negative control to establish the physiological specificity of the screen. Heat shock-inducible GFP-HA served as an internal control.

All experiments were repeated at least three times with similar results.

### Protein-Based Screens for Plant Endogenous MiRNA Targets

Many computational algorithms have been developed to predict endogenous targets for plant miRNAs, but facile and robust

experimental validation in plant cells remains limited and challenging due to the complexity of miRNA action mechanisms and the prevailing paucity of plant antibodies (Ossowski et al., 2008; Voinnet, 2009; Bonnet et al., 2010). We therefore extended the key concept of ETPamir screens to validate endogenous target

candidates of plant miRNAs. We used seven Web-based computational programs to predict endogenous target genes for the well-characterized *Arabidopsis* miR319a (see Supplemental Table 2 online). WMD and TAPIR (Bonnet et al., 2010) provided the most comprehensive list of potential target genes, among which we selected *TCP2*, *TCP10*, *TCP24*, and *ALDH22a1* for protein-based miRNA target screens. Considering miR319a was overexpressed in the screen, we also tested *TCP20*, a known untargeted *TCP* gene, as a negative control to establish the physiological specificity of the screen. Our data clearly validated *TCP2/10/24* but not *TCP20* as specific miR319a targets and excluded *ALDH22a1* predicted by WMD and TAPIR as an authentic miR319a target (Figures 6E and 6F). The silencing specificity of miR319a toward *TCP* genes and the ineffectiveness of nonfunctional variant miR319a<sup>129</sup> (Nag et al., 2009) in silencing any *TCP* gene (Figure 6F) confirmed that our ETP-based protoplast screens provided the same physiological target specificity as shown by independent studies in transgenic plants (Palatnik et al., 2003, 2007; Nag et al., 2009). Collectively, our data illustrated the power of the ETPamir screens for broad applications in plant research.

## DISCUSSION

We developed facile and versatile ETPamir screens that can identify amiRNAs with near 100% gene silencing efficacy within 3 h after target mRNA expression in protoplasts, which is remarkably rapid compared with 3 to 6 months generally required by transgenic analyses of amiRNA activities, even in *Arabidopsis*. The ETPamir screens quantify gene silencing under cellular and natural sequence and structural contexts by monitoring target protein levels, thus exceeding the accuracy of current routine methods, including the qRT-PCR/transcriptome approach (Schwab et al., 2006), which monitors target transcript levels, and the degradome method (Addo-Quaye et al., 2008), which relies on stable mRNA cleavage products. The ETPamir screens require no prior knowledge about target gene function and circumvent the complexity of amiRNA action mechanisms and unpredictable factors in amiRNA expression and processing. The use of an epitope tag in the screen also bypasses the current technical hurdle of plant antibody shortage and confers substantial sensitivity and flexibility.

Unlike rapidly dividing mammalian cell lines with dynamically changing nuclear state and ribosome biogenesis, which can

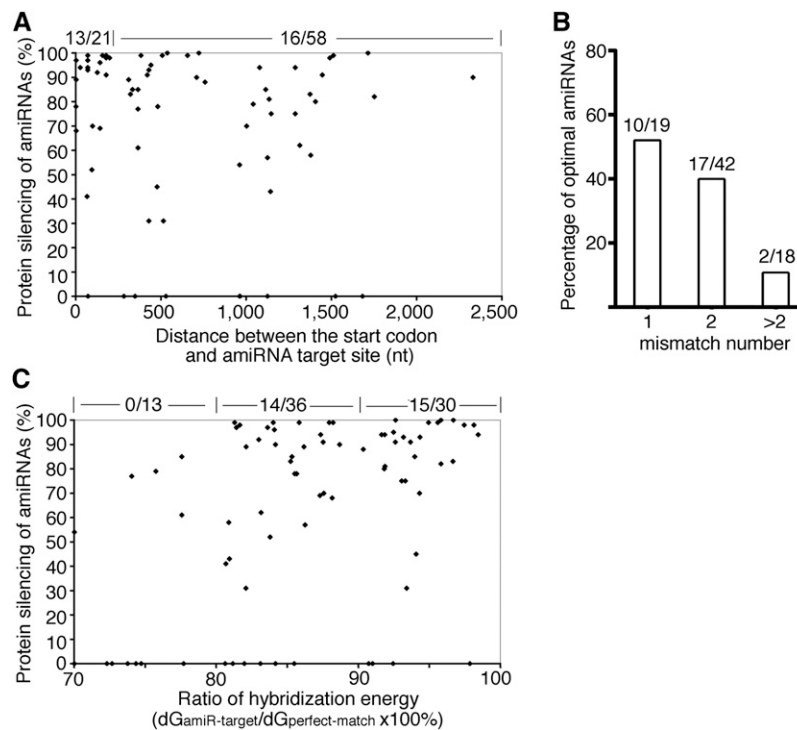


**Figure 7.** Analysis of the Distribution of Optimal AmiRNAs.

**(A)** Scatterplot of the amiRNA efficacy and the distance of amiRNA target site to the translation initiation site within target mRNAs. Optimal amiRNAs reach ~90% protein silencing efficacy (Table 1). The number of optimal amiRNAs versus the total number of candidates with the target site located <200 or >200 nucleotides (nt) from the start codon in the mRNA is shown at the top.

**(B)** Distribution of optimal amiRNAs among candidates with different mismatch numbers. The number of optimal amiRNAs versus the total number of candidates is shown on top of the column for the indicated mismatch number.

**(C)** Scatterplot of the ratio of hybridization energy ( $dG_{\text{amiR-target}}/dG_{\text{perfect-match}}$ ) of an amiRNA and its efficacy. The number of optimal amiRNAs versus the total number of candidates with the ratio of hybridization energy within 70 to 80%, 80 to 90%, or 90 to 100% is shown at the top.

interfere with gene silencing (Huntzinger and Izaurralde, 2011; Janas et al., 2012), the plant mesophyll protoplast system offers the advantages of high amiRNA silencing specificity (see Supplemental Figure 7 online), unlimited AGO activity (see Supplemental Figure 9 online), high cotransfection efficiency (Yoo et al., 2007), high-throughput potential (Li et al., 2011), and broad adaptability in numerous plant species (Sheen, 1991). In particular, our screens can be easily applied to diverse agronomically or pharmacologically important plant species (Figures 6C and 6D). The screens are especially valuable for genes such as *ANP2* and *LYM2*, which are relatively recalcitrant to amiRNA-mediated silencing (Table 1), and for multigene targets, for which an optimal amiRNA is more difficult to obtain (Figures 3B and 4A). Collectively, our findings demonstrate the advantages of conducting rapid ETPamir screens to identify optimal amiRNAs before undertaking laborious and time-consuming transgenic analyses.

Despite the presence of multiple miRNA target sites in 3' UTRs in animals (Chi et al., 2009; Guo et al., 2010; Huntzinger and Izaurralde, 2011; Pasquinelli, 2012), we found no evidence that targeting the 3' UTR of a plant gene could guarantee plant amiRNA an optimal silencing efficacy (Table 1; see Supplemental Figure 10A online). Our extensive analysis of target site accessibility using the Sfold server (Ding et al., 2004), a widely used prediction program, also failed to relate amiRNA performance to the predicted accessibility of the target region (see Supplemental Figure 11 online), as suggested by studies in *Caenorhabditis elegans* and *Drosophila melanogaster* (Long et al., 2007). Furthermore, our survey of 63 amiRNA candidates suggested no tight correlation between the WMD ranking of an amiRNA and the experimentally determined efficacy (Table 1; see Supplemental Figure 10B online).

Analysis of the distribution of optimal amiRNAs revealed a few trends that may guide future selection of optimal amiRNAs from the WMD output list. First, 13 out of 21 (62%) amiRNAs targeting the 5' 200 nucleotides of target gene CDS were found optimal,

and this percentage was significantly higher than that of amiRNAs aiming at other region of target genes (Figure 7A). These findings indicated that the inhibition of translation initiation might be an efficient mechanism for amiRNA-mediated gene silencing in plants. Second, the fewer mismatches an amiRNA has, the higher its probability of being an optimal amiRNA (Figure 7B). Third, the hybridization energy of an optimal amiRNA to its target ( $dG_{\text{amiR-target}}$ ) needs to reach >80% of that of the perfect match ( $dG_{\text{perfect-match}}$ ), even though the WMD applies  $dG_{\text{amiR-target}}/dG_{\text{perfect-match}}$  of 70% as the cutoff for amiRNA candidate design (Figure 7C). Based on these analyses, we suggest new criteria to select optimal amiRNA candidates from WMD outputs, including target site within the 5' 200 nucleotides of CDS, up to two mismatches at position 1 or 15 to 21, and with  $dG_{\text{amiR-target}}/dG_{\text{perfect-match}}$  above 80% (Figure 8A). Among all tested amiRNA candidates in 79 ETPamir screens, there were 17 candidates satisfying the new selection criteria (Table 1). Strikingly, 12 out of them (71%) were found to be optimal (Figure 8B). These new amiRNA selection rules can dramatically improve the identification of optimal amiRNAs from 15% (12/79) based on WMD to 71% (12/17) (Figure 8). Nevertheless, we would like to emphasize the critical and indispensable value of ETPamir screens for experimentally validating the most efficient amiRNA (Figure 8A), as the proper amiRNA expression and processing, the cellular context of amiRNA-target interaction, the target mRNA secondary structure, and target mRNA binding proteins could all affect the outcome of amiRNA-mediated gene silencing (Schwab et al., 2006; Ossowski et al., 2008; Bonnet et al., 2010; Huntzinger and Izaurralde, 2011; Pasquinelli, 2012).

In addition to its implementation in optimizing gene silencing in diverse plant species, we extended the ETPamir screen to study plant miRNA/amiRNA biology. Since the validation of natural plant miRNA targets is conceptually similar to the evaluation of target silencing for plant amiRNAs, we modified the rapid ETPamir screen as a convenient and robust tool to identify physiologically relevant

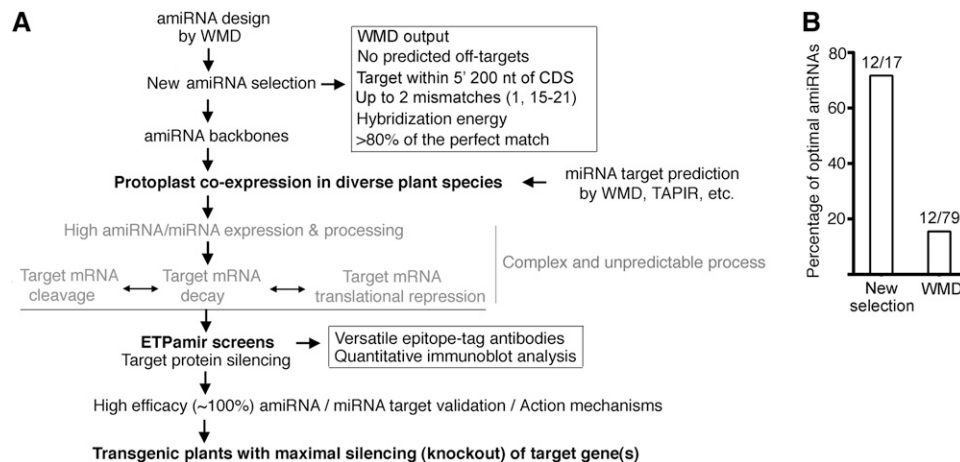


**Figure 8.** ETPamir Screens with New AmiRNA Selection Rules Facilitate Effective Gene Silencing in Plants.

**(A)** Guidelines for diverse applications of ETPamir screens in plant research.

**(B)** New selection rules dramatically improve the identification of optimal amiRNAs. Among amiRNA candidates tested in the 79 ETPamir screens, only 17 amiRNAs qualified the new selection rules **(A)**, and 12 (71%) out of these 17 amiRNAs conferred optimal protein silencing.

target genes for plant miRNAs (Figures 6F and 8A). This tool bypasses the uncertainty of miRNA action mechanisms and the shortage of specific plant antibodies and promises high-throughput validation of endogenous targets for plant miRNAs in the future.

Due to the limited availability of plant antibodies, there are very few studies on the kinetics and mechanisms of plant miRNA/amiRNA actions. Our strategy illustrated in Figure 5A can serve as a simple and valuable method for pinpointing plant miRNA/amiRNA action mechanisms. Although it is not possible to directly follow the abundance of an endogenous target protein without using a specific antibody, our analyses of MEKK1 proteins suggested that plant miRNA/amiRNA silences the endogenous target gene (encoding untagged protein) and the exogenously introduced target gene (encoding tagged protein) to the same extent (Figures 2 and 5E). Thus, the change in abundance of the tagged target protein can represent that of total (both tagged and untagged) target protein in real time, circumventing the requirement for specific antibodies. Currently, the prevailing model based on the near-perfect complementarity between plant miRNAs and their targets predicts that plant miRNAs and, by inference, plant amiRNAs predominantly trigger target mRNA cleavage and decay as the primary mechanism underlying gene silencing (Schwab et al., 2006; Mallory and Bouché, 2008). Surprisingly, our kinetic analysis revealed a significant translational repression and seemingly uncorrelated mRNA decay or cleavage by optimal amiRNAs (Figure 5E), supporting previous reports on translational inhibition by plant miRNAs (Aukerman and Sakai, 2003; Chen, 2004; Brodersen et al., 2008; Lanet et al., 2009).

Plant cells are distinct from animal cells in their high amiRNA specificity and potency. In future applications, several optimal amiRNAs with different target sequences in the same target gene can be identified using ETPamir screens to generate independent silencing lines. When necessary, amiRNA-resistant gene variants can complement these silencing lines to ensure silencing specificity and to establish solid gene-phenotype correlations. Our studies demonstrated that a single plant amiRNA on a single target site in the coding region of plant genes can achieve near 100% gene silencing and produce functionally null mutants (Figures 1 and 3, Table 1). This regulatory mechanism is different from animal miRNAs, which have clustered target sites in the 3' UTR with relaxed complementarity. The silencing efficacy detected for plant optimal amiRNAs has gone beyond the theoretical maximum (80%) of RNA silencing efficacy in mammalian cells (Silva et al., 2005). Taking advantage of the high effectiveness of the amiRNA technology, the ETPamir screens will greatly facilitate high-throughput systematic and genome-wide functional screens in diverse plant species.

## METHODS

### Plant Growth Conditions

Wild-type *Arabidopsis thaliana* Columbia-0 plants were grown on Jiffy7 soil (Jiffy Group) in a plant growth room with conditions maintained at 65% humidity and  $75 \mu\text{mol m}^{-2} \text{s}^{-1}$  light intensity under photoperiods of 12 h light at 23°C and 12 h dark at 20°C (Yoo et al., 2007). Tobacco (*Nicotiana benthamiana*), tomato (*Solanum lycopersicum*), sunflower (*Helianthus annuus*), and *Catharanthus roseus* plants were grown on Metro-Mix 360 soil (Sun Gro) under the same conditions as *Arabidopsis*.

Maize (*Zea mays*) plants, after germination for 3 d under light, were grown in a dark chamber for 7 d at 25°C and then exposed to  $30 \mu\text{mol m}^{-2} \text{s}^{-1}$  light for 12 h before protoplast isolation (Sheen, 1991). Rice (*Oryza sativa*) plants were grown on Fafard soil in a plant growth chamber with conditions maintained at 70% humidity and  $75 \mu\text{mol m}^{-2} \text{s}^{-1}$  light intensity under photoperiods of 12 h light at 28°C and 12 h dark at 26°C.

### Plasmid Construction

A total of 133 recombinant plasmids constructed during this study for transient or transgenic expression of amiRNAs or target genes are inventoried in Supplemental Table 3 and are available upon request. See Supplemental Methods 1 online for plasmid construction details. All plasmid DNA used for protoplast transfection was purified by CsCl gradient ultracentrifugation or homemade silica resin (Li et al., 2010).

### Protoplast Isolation and Transfection

Mesophyll protoplast isolation from leaves of 4-week-old *Arabidopsis* or tobacco, 3-week-old *C. roseus*, or 2-week-old tomato or sunflower was conducted as previously described (Yoo et al., 2007). Briefly, leaves were cut into 1-mm strips with a sterile razor blade and were digested in 10 mL of filtered enzyme solution (1.5% Cellulase R10, 0.4% macerozyme R10, 0.4 M mannitol, 20 mM KCl, 20 mM MES, pH 5.7, 10 mM  $\text{CaCl}_2$ , and 0.1% BSA) for 3 to 5 h with gentle shaking (40 rpm). After being filtered through a piece of Miracloth, protoplasts were pelleted by centrifugation at 1200 rpm for 2 min in a CL2 clinical centrifuge (Thermo Scientific) and were resuspended in 10 mL of W5 solution (154 mM NaCl, 125 mM  $\text{CaCl}_2$ , 5 mM KCl, and 2 mM MES, pH 5.7). After resting on ice for 30 min, protoplasts were spun down by centrifugation at 1200 rpm for 1 min in a CL2 centrifuge and were resuspended with MMg solution (0.4 M mannitol, 15 mM  $\text{MgCl}_2$ , and 4 mM MES, pH 5.7) to a final concentration of  $2 \times 10^5$  cells per mL. DNA transfection was performed in a 2-mL round-bottom microcentrifuge tube (or a 15-mL round-bottom tube for large amounts of protoplasts), where 200  $\mu\text{L}$  protoplasts ( $4 \times 10^4$  cells) were mixed with 21  $\mu\text{L}$  amiRNA/target gene-HA/internal control DNA cocktail. Polyethylene glycol (PEG) solution (220  $\mu\text{L}$  40% PEG [w/v], 0.2 M mannitol, and 0.1 M  $\text{CaCl}_2$ ) was added to each tube, and transfection was initiated sequentially by gentle tapping on the tube bottom to ensure complete mixture. After 5 min of incubation at room temperature, transfection was terminated in the same order by adding 800  $\mu\text{L}$  W5 solution and gently inverting the tube twice. Transfected protoplasts were harvested by centrifugation at 1200 rpm for 2 min in a CL2 centrifuge and were resuspended with 100  $\mu\text{L}$  W5 solution. The protoplasts were then transferred into 1 mL of WI solution (0.5 M mannitol, 4 mM MES, pH 5.7, and 20 mM KCl) in a six-well plate precoated with 5% fetal calf serum. Greening maize protoplasts were prepared as previously described (Sheen, 1991) and were transfected by electroporation. Protoplast isolation from 10-d-old rice green tissue and subsequent PEG-mediated transfection were conducted as previously described (Bart et al., 2006).

### ETPamir Screens for Optimal AmiRNA

Mesophyll protoplasts ( $4 \times 10^4$  cells in 200  $\mu\text{L}$ ) were transfected with 32  $\mu\text{g}$  (16  $\mu\text{L}$ ) of amiRNA constructs and 8  $\mu\text{g}$  (4  $\mu\text{L}$ ) of target gene-HA constructs (Figure 1A). In parallel, 32  $\mu\text{g}$  of empty amiRNA expression vector and 8  $\mu\text{g}$  of target gene-HA constructs were cotransfected as a control to indicate target gene expression without amiRNA silencing. GFP-HA/LUC constructs (2  $\mu\text{g}$  in 1  $\mu\text{L}$ ) were cotransfected in all cases as a transfection internal control. Transfected cells were resuspended with 100  $\mu\text{L}$  W5 solution and transferred to 1 mL WI solution in a six-well plate. For protoplast incubation over 24 h, the transfer step was performed in a sterile hood and 100  $\mu\text{g}/\text{mL}$  of ampicillin was supplemented to inhibit bacterial growth (Kim and Somers, 2010). The plate was incubated under

normal plant growth conditions (Yoo et al., 2007). Cells can be harvested at different time points to determine the efficacy of amiRNA action. The empirically determined optimal time to harvest cells for most of the target proteins was 36 h after cotransfection. For unstable target proteins, a shorter incubation time (e.g., 6 to 12 h after cotransfection) was used. Pelleted protoplasts were lysed in 40  $\mu$ L of SDS loading buffer at 95°C for 5 min. Total proteins were subjected to SDS-PAGE and immunoblot analysis using anti-HA HRP-conjugated antibodies (Sigma-Aldrich) at 1:10,000 dilution. Immunoblot signals (36 h) were quantified by densitometric analysis using the Image J program (NIH) for calculating the silencing efficiency.

#### Analysis of AmiRNA Action Mechanism and Kinetics

Mesophyll protoplasts ( $2 \times 10^5$  cells in 1 mL) were transfected with 180  $\mu$ g (90  $\mu$ L) of amiRNA constructs and 20  $\mu$ g (10  $\mu$ L) of heat shock promoter (*HSP*)-driven target gene-HA constructs (Figure 5A). In parallel, 180  $\mu$ g of empty amiRNA expression vector and 20  $\mu$ g of *HSP*-driven target gene-HA constructs were cotransfected as a control to indicate target gene expression without amiRNA silencing. *HSP*-driven GFP-HA/LUC constructs (10  $\mu$ g in 5  $\mu$ L) were cotransfected in all cases as a transfection internal control. Transfected cells were resuspended with 500  $\mu$ L W5 solution and transferred to 5 mL of WI solution in a 100 mm  $\times$  20-mm Petri dish. The protoplasts were incubated for 3 h at room temperature before the heat shock pulse at 37°C for 1 h. Cells were harvested for qRT-PCR analysis of target mRNAs (80% cells) after 1 h incubation at room temperature and for immunoblot analysis of target protein (20% cells) after 3 h incubation at room temperature. To rapidly identify the optimal amiRNA for a target gene or to validate predicted plant miRNA targets, 32  $\mu$ g (16  $\mu$ L) of amiRNA/miRNA constructs and 8  $\mu$ g (4  $\mu$ L) of *HSP*-driven target gene-HA constructs were used to transfect protoplasts ( $4 \times 10^4$  cells in 200  $\mu$ L), and the same procedure for immunoblot analysis was followed.

#### RNA Isolation and qRT-PCR

Total RNA was extracted from *Arabidopsis* protoplasts or seedlings using the Trizol reagent (Invitrogen). After DNase I (Roche) treatment, total RNA (1  $\mu$ g) were used for cDNA synthesis with the ImPromII reverse transcriptase (Promega) according to the manufacturer's instruction. Quantitative PCR was performed in a CFX96 real-time system (Bio-Rad) using iQ SYBR Green Supermix (Bio-Rad). *UBQ10* was used as internal control. Primers used for quantitative PCR in this study are listed in Supplemental Table 4 online.

#### RNA Blot Analysis for AmiRNA Expression

Total RNA (15 g) isolated from protoplasts expressing individual amiRNAs for 6 hr were resolved in a 15% polyacrylamide / 8 M urea denaturing gel and transferred to a Hybond N+ nitrocellulose membrane (GE healthcare). One pmol of DNA oligonucleotides with complementary sequences to the corresponding amiRNAs (see Supplemental Table 5 online) were end-labeled with P-32 using T4 polynucleotide kinase (Thermo Scientific) and purified through QIAquick nucleotide removal kit (QIAGEN) to generate specific probes. Hybridization was performed at 45°C in church buffer (0.5 M NaPO<sub>4</sub>, 7% SDS, 1 mM EDTA, 1% BSA, pH 7.5) for 16 hr. The membranes were exposed to a phosphorimager screen and radioactive signals were recorded by the Typhoon phosphorimager (GE healthcare).

#### Generation of Transgenic Plants

The recombinant binary plasmids were introduced into *Agrobacterium tumefaciens* strain GV3101 through electroporation. Transgenic *Arabidopsis* was generated through the floral dip method (Clough and Bent, 1998).

Transgenic plants were selected in soil presoaked with Finale herbicides (Farnam Companies) containing glufosinate ammonium.

#### Accession Numbers

Sequence data from this article can be found in the Arabidopsis Genome Initiative or GenBank/EMBL databases under the following accession numbers: *MEKK1*, At4g08500; *YDA*, At1g63700; *ALPHA*, At1g53570; *GAMMA*, At5g66850; *ANP1*, At1g09000; *ANP2*, At1g54960; *ANP3*, At3g06030; *MAPKKK17*, At2g32510; *MAPKKK18*, At1g05100; *LYM2*, At2g17120; *PDS3*, At4g14210; *ZAT6*, At5g04340; *RACK1a*, At1G18080; *RACK1b*, At1g48630; *RACK1c*, At3g18130; *AGO1*, At1g48410; *AGO2*, At1g31280; *AGO4*, At2g27040; *AGO10*, At5g43810; *TCP2*, At4g18390; *TCP10*, At2g31070; *TCP20*, At3g27010; *TCP24*, At1g30210; *ALDH22a1*, At3g66658; and *UBQ10*, At4g05320.

#### Supplemental Data

The following materials are available in the online version of this article.

**Supplemental Figure 1.** WMD-Predicted AmiRNA Candidates for Single-Gene Silencing.

**Supplemental Figure 2.** ETPamir Screens of Optimal AmiRNAs for Other Single Gene Silencing in *Arabidopsis*.

**Supplemental Figure 3.** WMD-Predicted AmiRNA Candidates for Multigene Silencing.

**Supplemental Figure 4.** RNA Gel Blot Analysis of AmiRNA Expression.

**Supplemental Figure 5.** WMD-Predicted AmiRNA Candidates for Silencing Individual Members of the *MAPKKK YDA* Family.

**Supplemental Figure 6.** In Planta Validation of AmiRNA-Mediated Gene Silencing by Tobacco Leaf Agroinfiltration.

**Supplemental Figure 7.** ETPamir Screens Reveal High Specificity of Gene Silencing by Plant AmiRNAs.

**Supplemental Figure 8.** Limited Cross-Species Activity of *Arabidopsis* miR319a-Derived AmiRNA and Rice miR528-Derived AmiRNA.

**Supplemental Figure 9.** Unlimited Argonaute Activity in *Arabidopsis* Mesophyll Protoplasts.

**Supplemental Figure 10.** No Tight Correlation between the 3' UTR Targeting or WMD Ranking of an AmiRNA and Its Efficacy.

**Supplemental Figure 11.** Visual Summary of AmiRNA/miRNA Target Site Location, Predicted Target Accessibility, and Target Complementarity.

**Supplemental Table 1.** Summary of AmiRNAs for Silencing the *MAPKKK YDA* Family.

**Supplemental Table 2.** Predicted Natural Target Genes for *Arabidopsis* miR319a.

**Supplemental Table 3.** Recombinant Plasmids Constructed during This Study.

**Supplemental Table 4.** Primers Used for qPCR in This Study.

**Supplemental Table 5.** Sequences of AmiRNA/miRNAs Tested during This Study.

**Supplemental Methods 1.** Detailed Procedures for Plasmid Construction, Agroinfiltration, and Bioinformatics Analyses.

#### ACKNOWLEDGMENTS

We thank Frederick Ausubel for critical reading of the article, Detlef Weigel and Rebecca Schwab for the WMD platform, Jin-Gui Chen for the

T-DNA insertion *rack1* null mutants, Carolyn Lee-Parsons for *C. roseus* plants, Mark Curtis and Ueli Grossniklaus for the estradiol-inducible binary vector, and the ABRC for the *mekk1* and *pds3* mutants. We also thank Guillaume Tena for the original miR319a plasmid, Li Li for maize protoplast transfection, and Qi Hall for assistance in floral dip. J.-F.L. is supported by the Massachusetts General Hospital Executive Committee on Research Postdoctoral Fellowship for Medical Discovery. The research is supported by National Science Foundation Grant IOS-0843244 and the National Institutes of Health Grants R01 GM60493 and R01 GM70567 to J.S.

#### AUTHOR CONTRIBUTIONS

J.-F.L. conceived and designed the experiments, performed the majority of the experiments, analyzed the data, and wrote the article. H.S.C. performed the ETPamir screen for amiR-ZAT6s and the RNA blot analysis. Y.N. performed the live-cell imaging. J.B. prepared plants for protoplast isolation. M.M. performed bioinformatics analyses. J.S. designed the experiments and wrote the article. All authors read and approved the final article.

Received April 2, 2013; revised April 2, 2013; accepted April 20, 2013; published May 3, 2013.

#### REFERENCES

- Addo-Quaye, C., Eshoo, T.W., Bartel, D.P., and Axtell, M.J.** (2008). Endogenous siRNA and miRNA targets identified by sequencing of the *Arabidopsis* degradome. *Curr. Biol.* **18**: 758–762.
- Alvarez, J.P., Pekker, I., Goldshmidt, A., Blum, E., Amsellem, Z., and Eshed, Y.** (2006). Endogenous and synthetic microRNAs stimulate simultaneous, efficient, and localized regulation of multiple targets in diverse species. *Plant Cell* **18**: 1134–1151.
- Aukerman, M.J., and Sakai, H.** (2003). Regulation of flowering time and floral organ identity by a microRNA and its APETALA2-like target genes. *Plant Cell* **15**: 2730–2741.
- Bart, R., Chern, M., Park, C.J., Bartley, L., and Ronald, P.C.** (2006). A novel system for gene silencing using siRNAs in rice leaf and stem-derived protoplasts. *Plant Methods* **2**: 13.
- Bonnet, E., He, Y., Billiau, K., and Van de Peer, Y.** (2010). TAPIR, a web server for the prediction of plant microRNA targets, including target mimics. *Bioinformatics* **26**: 1566–1568.
- Brodersen, P., Sakvarelidze-Achard, L., Bruun-Rasmussen, M., Dunoyer, P., Yamamoto, Y.Y., Sieburth, L., and Voinnet, O.** (2008). Widespread translational inhibition by plant miRNAs and siRNAs. *Science* **320**: 1185–1190.
- Chen, X.** (2004). A microRNA as a translational repressor of APETALA2 in *Arabidopsis* flower development. *Science* **303**: 2022–2025.
- Chi, S.W., Zang, J.B., Mele, A., and Darnell, R.B.** (2009). Argonaute HITS-CLIP decodes microRNA-mRNA interaction maps. *Nature* **460**: 479–486.
- Clough, S.J., and Bent, A.F.** (1998). Floral dip: A simplified method for *Agrobacterium*-mediated transformation of *Arabidopsis thaliana*. *Plant J.* **16**: 735–743.
- Ding, Y., Chan, C.Y., and Lawrence, C.E.** (2004). Sfold web server for statistical folding and rational design of nucleic acids. *Nucleic Acids Res.* **32** (Web Server issue): W135–W141.
- Dugas, D.V., and Bartel, B.** (2008). Sucrose induction of *Arabidopsis* miR398 represses two Cu/Zn superoxide dismutases. *Plant Mol. Biol.* **67**: 403–417.
- Fabian, M.R., Sonenberg, N., and Filipowicz, W.** (2010). Regulation of mRNA translation and stability by microRNAs. *Annu. Rev. Biochem.* **79**: 351–379.
- Fukaya, T., and Tomari, Y.** (2012). MicroRNAs mediate gene silencing via multiple different pathways in *Drosophila*. *Mol. Cell* **48**: 825–836.
- Gandikota, M., Birkenbihl, R.P., Höhmann, S., Cardon, G.H., Saedler, H., and Huijser, P.** (2007). The miRNA156/157 recognition element in the 3' UTR of the *Arabidopsis* SBP box gene SPL3 prevents early flowering by translational inhibition in seedlings. *Plant J.* **49**: 683–693.
- Guo, H., Ingolia, N.T., Weissman, J.S., and Bartel, D.P.** (2010). Mammalian microRNAs predominantly act to decrease target mRNA levels. *Nature* **466**: 835–840.
- Guo, J., and Chen, J.G.** (2008). RACK1 genes regulate plant development with unequal genetic redundancy in *Arabidopsis*. *BMC Plant Biol.* **8**: 108.
- Huntzinger, E., and Izaurralde, E.** (2011). Gene silencing by microRNAs: Contributions of translational repression and mRNA decay. *Nat. Rev. Genet.* **12**: 99–110.
- Janas, M.M., et al.** (2012). Reduced expression of ribosomal proteins relieves microRNA-mediated repression. *Mol. Cell* **46**: 171–186.
- Kim, J., and Somers, D.E.** (2010). Rapid assessment of gene function in the circadian clock using artificial microRNA in *Arabidopsis* mesophyll protoplasts. *Plant Physiol.* **154**: 611–621.
- Lanet, E., Delannoy, E., Sormani, R., Floris, M., Brodersen, P., Crété, P., Voinnet, O., and Robaglia, C.** (2009). Biochemical evidence for translational repression by *Arabidopsis* microRNAs. *Plant Cell* **21**: 1762–1768.
- Li, J.F., Bush, J., Xiong, Y., Li, L., and McCormack, M.** (2011). Large-scale protein-protein interaction analysis in *Arabidopsis* mesophyll protoplasts by split firefly luciferase complementation. *PLoS ONE* **6**: e27364.
- Li, J.F., Li, L., and Sheen, J.** (2010). Protocol: A rapid and economical procedure for purification of plasmid or plant DNA with diverse applications in plant biology. *Plant Methods* **6**: 1.
- Long, D., Lee, R., Williams, P., Chan, C.Y., Ambros, V., and Ding, Y.** (2007). Potent effect of target structure on microRNA function. *Nat. Struct. Mol. Biol.* **14**: 287–294.
- Mallory, A.C., and Bouché, N.** (2008). MicroRNA-directed regulation: To cleave or not to cleave. *Trends Plant Sci.* **13**: 359–367.
- MAPK Group** (2002). Mitogen-activated protein kinase cascades in plants: A new nomenclature. *Trends Plant Sci.* **7**: 301–308.
- Merchan, F., Boualem, A., Crespi, M., and Frugier, F.** (2009). Plant polycistronic precursors containing non-homologous microRNAs target transcripts encoding functionally related proteins. *Genome Biol.* **10**: R136.
- Miranda, K.C., Huynh, T., Tay, Y., Ang, Y.S., Tam, W.L., Thomson, A.M., Lim, B., and Rigoutsos, I.** (2006). A pattern-based method for the identification of MicroRNA binding sites and their corresponding heteroduplexes. *Cell* **126**: 1203–1217.
- Nag, A., King, S., and Jack, T.** (2009). miR319a targeting of TCP4 is critical for petal growth and development in *Arabidopsis*. *Proc. Natl. Acad. Sci. USA* **106**: 22534–22539.
- Nakagami, H., Soukupová, H., Schikora, A., Zárský, V., and Hirt, H.** (2006). A mitogen-activated protein kinase kinase kinase mediates reactive oxygen species homeostasis in *Arabidopsis*. *J. Biol. Chem.* **281**: 38697–38704.
- Niu, Q.W., Lin, S.S., Reyes, J.L., Chen, K.C., Wu, H.W., Yeh, S.D., and Chua, N.H.** (2006). Expression of artificial microRNAs in transgenic *Arabidopsis thaliana* confers virus resistance. *Nat. Biotechnol.* **24**: 1420–1428.
- O'Malley, R.C., and Ecker, J.R.** (2010). Linking genotype to phenotype using the *Arabidopsis* unimutant collection. *Plant J.* **61**: 928–940.
- Ossowski, S., Schwab, R., and Weigel, D.** (2008). Gene silencing in plants using artificial microRNAs and other small RNAs. *Plant J.* **53**: 674–690.

- Palatnik, J.F., Allen, E., Wu, X., Schommer, C., Schwab, R., Carrington, J.C., and Weigel, D.** (2003). Control of leaf morphogenesis by microRNAs. *Nature* **425**: 257–263.
- Palatnik, J.F., Wollmann, H., Schommer, C., Schwab, R., Boisbouvier, J., Rodriguez, R., Warthmann, N., Allen, E., Dezulian, T., Huson, D., Carrington, J.C., and Weigel, D.** (2007). Sequence and expression differences underlie functional specialization of *Arabidopsis* microRNAs miR159 and miR319. *Dev. Cell* **13**: 115–125.
- Parizotto, E.A., Dunoyer, P., Rahm, N., Himber, C., and Voinnet, O.** (2004). In vivo investigation of the transcription, processing, endonucleolytic activity, and functional relevance of the spatial distribution of a plant miRNA. *Genes Dev.* **18**: 2237–2242.
- Park, W., Zhai, J., and Lee, J.Y.** (2009). Highly efficient gene silencing using perfect complementary artificial miRNA targeting AP1 or heteromeric artificial miRNA targeting AP1 and CAL genes. *Plant Cell Rep.* **28**: 469–480.
- Pasquinelli, A.E.** (2012). MicroRNAs and their targets: Recognition, regulation and an emerging reciprocal relationship. *Nat. Rev. Genet.* **13**: 271–282.
- Qin, G., Gu, H., Ma, L., Peng, Y., Deng, X.W., Chen, Z., and Qu, L.J.** (2007). Disruption of phytoene desaturase gene results in albino and dwarf phenotypes in *Arabidopsis* by impairing chlorophyll, carotenoid, and gibberellin biosynthesis. *Cell Res.* **17**: 471–482.
- Ren, D., Liu, Y., Yang, K.Y., Han, L., Mao, G., Glazebrook, J., and Zhang, S.** (2008). A fungal-responsive MAPK cascade regulates phytoalexin biosynthesis in *Arabidopsis*. *Proc. Natl. Acad. Sci. USA* **105**: 5638–5643.
- Sablok, G., Pérez-Quintero, A.L., Hassan, M., Tatarinova, T.V., and López, C.** (2011). Artificial microRNAs (amiRNAs) engineering - On how microRNA-based silencing methods have affected current plant silencing research. *Biochem. Biophys. Res. Commun.* **406**: 315–319.
- Schwab, R., Ossowski, S., Riester, M., Warthmann, N., and Weigel, D.** (2006). Highly specific gene silencing by artificial microRNAs in *Arabidopsis*. *Plant Cell* **18**: 1121–1133.
- Schwab, R., Palatnik, J.F., Riester, M., Schommer, C., Schmid, M., and Weigel, D.** (2005). Specific effects of microRNAs on the plant transcriptome. *Dev. Cell* **8**: 517–527.
- Sheen, J.** (1991). Molecular mechanisms underlying the differential expression of maize pyruvate, orthophosphate dikinase genes. *Plant Cell* **3**: 225–245.
- Silva, J.M., et al.** (2005). Second-generation shRNA libraries covering the mouse and human genomes. *Nat. Genet.* **37**: 1281–1288.
- Voinnet, O.** (2009). Origin, biogenesis, and activity of plant microRNAs. *Cell* **136**: 669–687.
- Warthmann, N., Chen, H., Ossowski, S., Weigel, D., and Herve, P.** (2008). Highly specific gene silencing by artificial miRNAs in rice. *PLoS ONE* **3**: e1829.
- Yoo, S.D., Cho, Y.H., and Sheen, J.** (2007). *Arabidopsis* mesophyll protoplasts: A versatile cell system for transient gene expression analysis. *Nat. Protoc.* **2**: 1565–1572.
- Zeng, Y., Wagner, E.J., and Cullen, B.R.** (2002). Both natural and designed micro RNAs can inhibit the expression of cognate mRNAs when expressed in human cells. *Mol. Cell* **9**: 1327–1333.
- Zuo, J., Niu, Q.W., and Chua, N.H.** (2000). Technical advance: An estrogen receptor-based transactivator XVE mediates highly inducible gene expression in transgenic plants. *Plant J.* **24**: 265–273.